

## Hadronic light-by-light contribution to muon $g - 2$

---

**Luchang Jin**<sup>a,b,\*</sup>

<sup>a</sup>*Physics Department, University of Connecticut,  
Storrs, Connecticut 06269-3046, USA*

<sup>b</sup>*RIKEN BNL Research Center, Brookhaven National Laboratory,  
Upton, New York 11973, USA*

*E-mail:* [ljin.luchang@gmail.com](mailto:ljin.luchang@gmail.com)

Recent lattice QCD results for hadron light-by-light scattering (HLbL) and its contribution to muon anomalous magnetic moments ( $g - 2$ ) will be reviewed. Combining the first results from Fermilab's Muon  $g - 2$  measurement and the previous BNL Muon  $g - 2$  experiment, there are currently 4.2 standard deviations between the experimental result and the theoretical prediction. The precision of Fermilab's experimental result will continue to improve in the coming years as more data is being analyzed. The uncertainty of theory prediction needs to be reduced to a similar level. Theoretically, HLbL and hadron vacuum polarization (HVP) contributions are the two major sources of uncertainty. In the past, the HLbL was only estimated by models. Recent developments in lattice calculations and data-driven approaches allow a reliable and systematically improvable determination of the HLbL contribution muon  $g - 2$ .

*The 10th International Workshop on Chiral Dynamics - CD2021  
15-19 November 2021  
Online*

---

\*Speaker

### 1. Introduction

Muon anomalous magnetic moments is one of the most precisely measured physical observables. The dimensionless number,  $a_\mu = (g - 2)/2$ , is defined through the following relation:

$$\vec{\mu} = 2(1 + a_\mu) \frac{-e}{2m_\mu} \vec{s} \tag{1}$$

where  $\vec{\mu}$  is the magnetic moment of muon and  $\vec{s}$  is its spin. The value of  $a_\mu$  can be calculated theoretically using quantum field theory through the photon-muon vertex function:

$$\bar{u}(p') [F_1(q^2)\gamma_\nu + iF_2(q^2)[\gamma_\nu, \gamma_\rho]q_\rho / (4m_\mu)] u(p), \tag{2}$$

and  $a_\mu = F_2(q^2 = 0)$ . The diagram for the photon-muon vertex is Fig. 1 left. At leading order,  $a_\mu$  is given by the 1-loop diagram, Fig. 1 right.

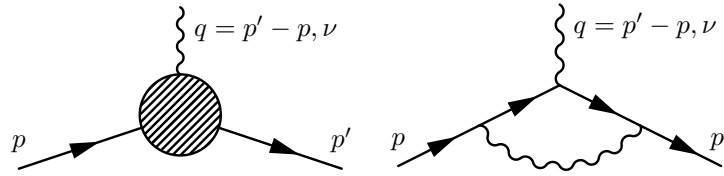


**Figure 1:** Left: photon-muon vertex. Right: leading contribution to muon anomalous magnetic moments,  $a_\mu = \alpha / (2\pi) = 11614097.3242 \times 10^{-10}$  [1].

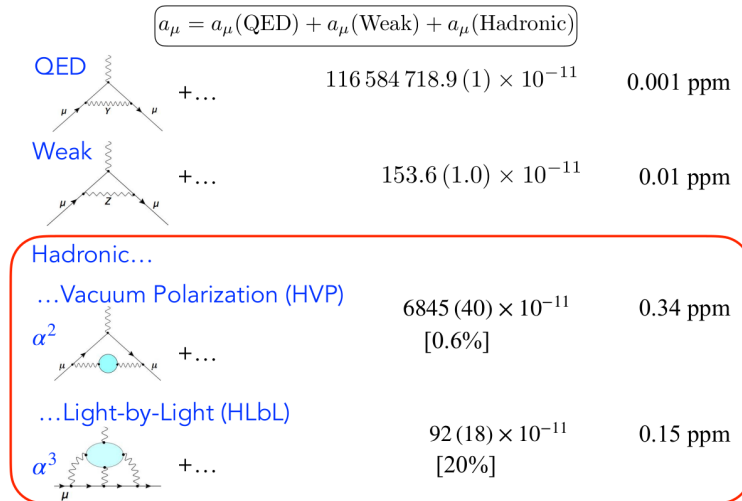


**Figure 2:** Figure from Aida El-Khadra’s theory talk during the Fermilab  $g - 2$  result announcement.

The theoretically prediction of muon anomalous magnetic moment recommended by the Muon  $g - 2$  Theory Initiative White paper [2] is

$$a_\mu^{\text{theory}} = 116 591 810(43) \times 10^{-11}. \tag{3}$$

This result is the sum of the contributions from the three fundamental interactions as shown in Figure 2. The QED contribution to the muon  $g - 2$  can be calculated perturbatively and has been calculated to 5-loops order [3], the weak contribution is also studied to 2-loops order [4]. The hadronic light-by-light and the hadronic vacuum polarization are the two contributions that involve the hadronic interaction. These two are currently the major sources of theoretical uncertainties.

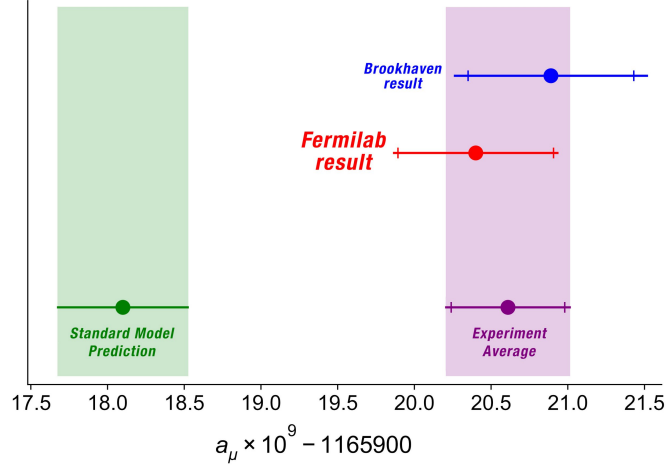


**Figure 3:** Experimental results from BNL E821 [5] and Fermilab E989 [6–9] results compared with the theoretically prediction recommended by the Muon  $g - 2$  Theory Initiative White paper [2].

At present, there are 4.2 standard deviation tension between the theory prediction [2] and the experimental measurements [5, 6], as shown in Figure 3. Beside the current Fermilab’s experimental effort, a J-PARC experiment aims to measure  $a_\mu$  and the electric dipole moment (EDM) in a completely different way, by using a low-emittance muon beam realized by acceleration of the thermal muons. [10, 11]

This quite significant deviation motivate further improvements in reducing the uncertainties of the theoretical prediction of muon  $g - 2$ . For a very long time, the HLbL contribution is estimated by models. Its value is  $a_\mu^{\text{HLbL}} = 105(26) \times 10^{-11}$  [12] known as the “Glasgow consensus”. There are also other compilations of models for HLbL. [13, 14] They all obtain similar values. In the last few years, many significant developments have been made in the data-driven analytical approaches. [15–26, 32] In the white paper,  $a_\mu^{\text{HLbL}} = 92(19) \times 10^{-11}$  [2] is obtained. While further improve the precision along this line is increasingly challenging, recent work shows that it should be possible to achieve this goal with a combination of rigorous short-distance constraints and experimental input [27–31] on the sub-leading intermediate states. [32]

Lattice QCD calculation provide another systematically improvable method to obtain the HLbL contribution to muon  $g - 2$ . The HLbL diagrams for lattice QCD calculations are shown in Figure 4. Gluons and sea quark loops (not directly connected to photons) are included automatically to all orders in lattice calculations and are not drawn explicitly in the figure. We will refer to the diagrams with multiple quark loops, which are connected by gluons that are not drawn in the figure, as the

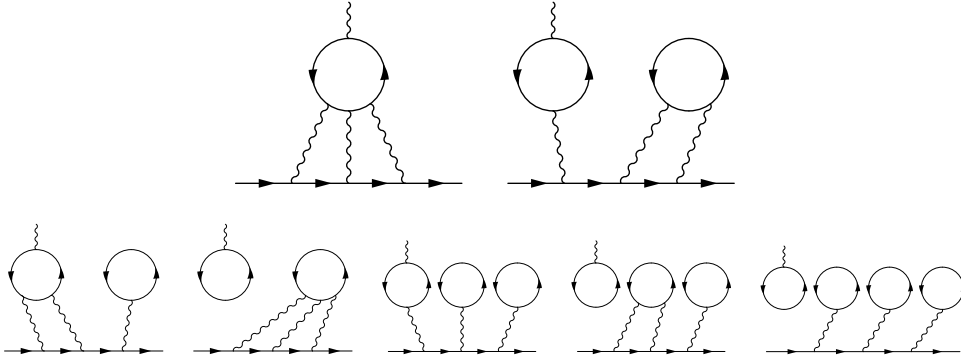


**Figure 4:** HLbL diagrams in lattice calculation. For each of the above diagrams, there are other possible permutations of the connections between the three internal photons and the muon line that are not shown. The first row shows the only two type of diagrams which do not vanish in the flavor SU(3) limit.

disconnected diagrams. At present, there are two independent lattice results available:

$$a_{\mu}^{\text{HLbL}} = 78.7(30.6)_{\text{stat}}(17.7)_{\text{sys}} \times 10^{-11} \quad (4)$$

from the RBC-UKQCD collaborations using the QED<sub>L</sub> approach. [33]

$$a_{\mu}^{\text{HLbL}} = 106.8(11.5)_{\text{stat}}(11.0)_{\text{sys}} \times 10^{-11} \quad (5)$$

from the Mainz collaboration using the QED<sub>∞</sub> approach. [34] We will discuss these two results in more details in the following sections. The combination of analytical approach and lattice QCD results from RBC/UKQCD (and adding the c-loop contribution) leads to the final recommendation of the white paper  $a_{\mu}^{\text{HLbL}} = 90(17) \times 10^{-11}$ . [2]

## 2. QED<sub>L</sub> approach

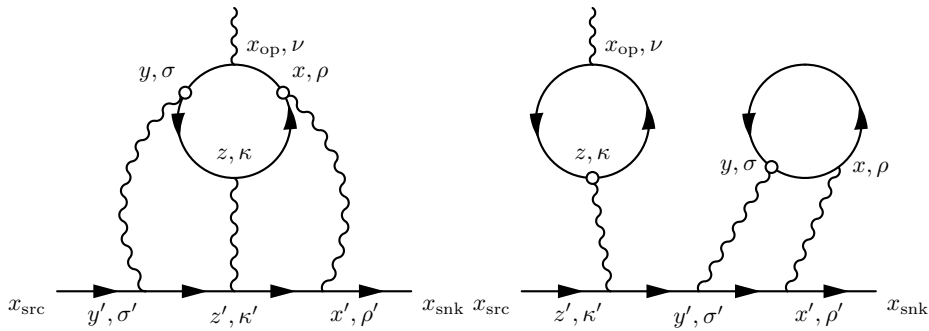


**Figure 5:** Small open circle represent the point source locations. Different permutations of the connections between the three internal vertices and the muon line are shown but included in the calculation.

The HLbL diagrams as shown in Figure 4 involves both QCD and QED interactions. Lattice method treat the QCD interactions in a finite periodic Euclidean space-time volume. QED<sub>L</sub>

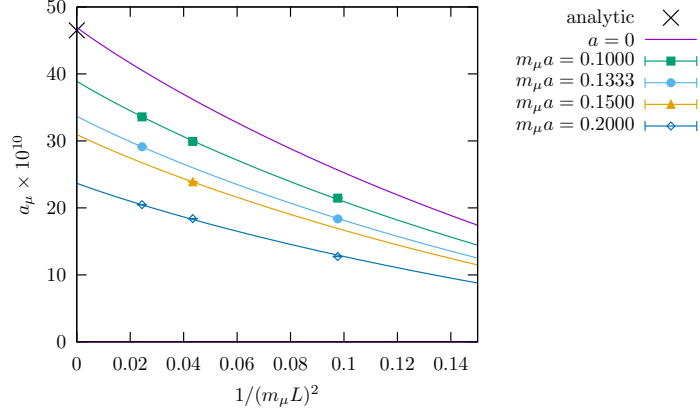


**Figure 6:** QED light-by-light scattering contribution from the muon loop to the muon  $g - 2$ . [33, 38]

	48I	64I	24D	32D	48D	32Dfine
$a^{-1}$ (GeV)	1.730	2.359	1.015	1.015	1.015	1.378
$a$ (fm)	0.114	0.084	0.194	0.194	0.194	0.143
$L$ (fm)	5.47	5.38	4.67	6.22	9.33	4.58
$L_s$	48	64	24	24	24	32
$m_\pi$ (MeV)	139	135	142	142	142	144
$m_\mu$ (MeV)	106	106	106	106	106	106
# meas con	65	43	157	70	8	75
# meas discon	124	105	156	69	0	69

**Table 1:** 2+1 flavors of MDWF gauge field ensembles generated by the RBC/UKQCD collaborations [40]. The lattice spacing  $a$ , spatial extent  $L$ , extra fifth dimension size  $L_s$ , muon pion mass  $m_\pi$ , and number of QCD configuration used for the connected and the disconnected diagrams.

is a common scheme to include QED interaction in a finite volume lattice. [37] The first lattice calculation of HLbL is performed by the RBC-UKQCD collaboration using the  $\text{QED}_L$  scheme. [35] A carefully designed subtraction method [36] is used to calculate the rather complicated HLbL diagram via the difference of two much simpler diagrams. A series improvements in methodology were made later to allow a more direct and efficient evaluation of the diagrams. [38] Random sampling of the point source quark propagators is used as is illustrated in Figure 5, where the small open circles denote the locations of the point sources. Importance sampling is used to focus on the small  $|x - y|$  region and complete sampling is performed for  $|x - y| \leq 5a$  up to discrete symmetry. The HLbL contribution is can be calculated based on the evaluation of the amplitude of the diagram via the following master equation:

$$\frac{a_\mu}{m_\mu} \bar{u}_{s'}(\vec{0}) \frac{\Sigma}{2} u_s(\vec{0}) = \sum_{r=x-y} \sum_z \sum_{x_{\text{op}}} \frac{1}{2} (\vec{x}_{\text{op}} - \vec{x}_{\text{ref}}) \times \bar{u}_{s'}(\vec{0}) i \vec{\mathcal{F}}^C(\vec{0}; x, y, z, x_{\text{op}}) u_s(\vec{0}), \quad (6)$$

where  $\vec{\mathcal{F}}^C$  represent the amplitude of the diagram before summation over the four photon quark

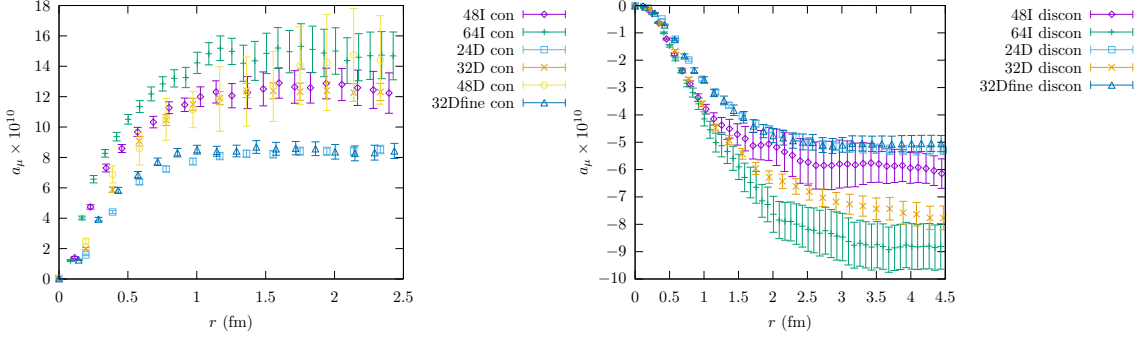


**Figure 7:** Cumulative contributions to the muon anomaly, connected (upper) and disconnected (lower).  $r$  is the distance between the two sampled currents in the hadronic loop (the other two currents are summed exactly). [33]

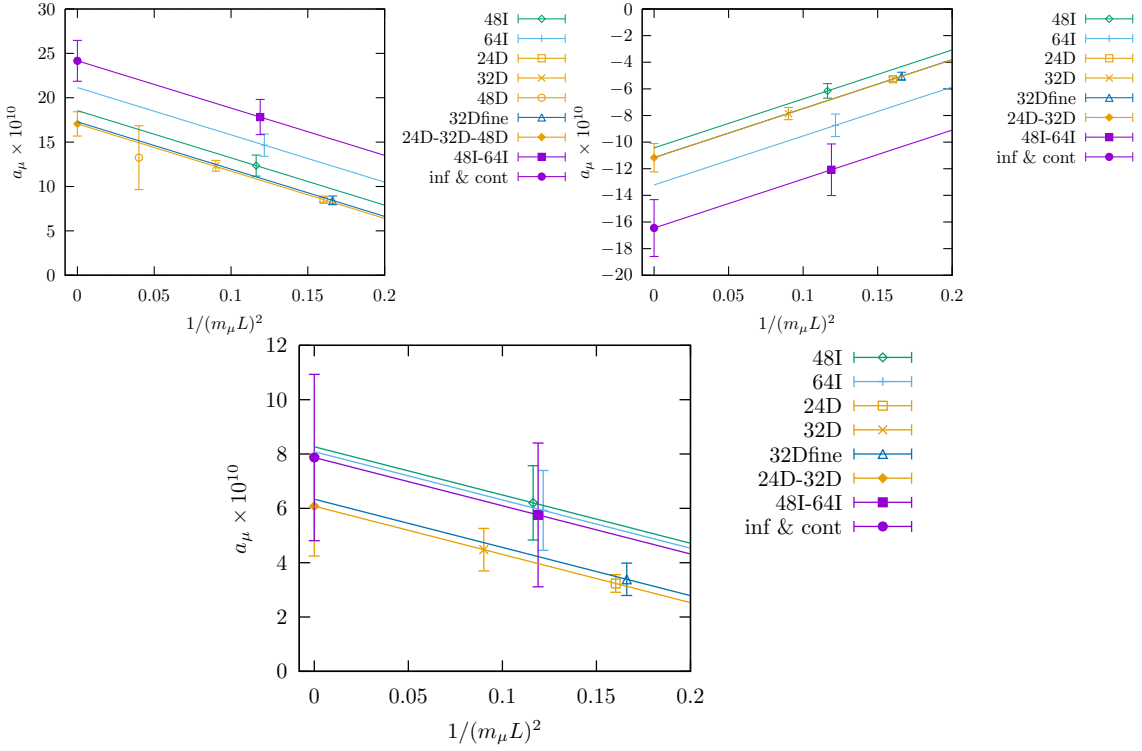


**Figure 8:** Infinite volume extrapolation. Connected (top), disconnected (middle), and total (bottom). We have use the hybrid method to calculate the continuum limit for the connected contribution. [33]

vertices. The formula is similar to the classical formula to obtain the magnetic moment:

$$\vec{\mu} = \sum_{\vec{x}_{\text{op}}} \frac{1}{2} (\vec{x}_{\text{op}} - \vec{x}_{\text{ref}}) \times \vec{J}(\vec{x}_{\text{op}}). \quad (7)$$

There are three subtle differences listed below which allows an efficient evaluation of the diagram in a finite volume lattice.

- Muon is plane wave,  $x_{\text{ref}} = (x + y)/2$ .

	con	discon	tot
$a_\mu$	24.16(2.30)	-16.45(2.13)	7.87(3.06)
sys hybrid $\mathcal{O}(a^2)$	0.20(0.45)	0	0.20(0.45)
sys $\mathcal{O}(1/L^3)$	2.34(0.41)	1.72(0.32)	0.83(0.56)
sys $\mathcal{O}(a^4)$	0.88(0.31)	0.71(0.28)	0.95(0.92)
sys $\mathcal{O}(a^2 \log(a^2))$	0.23(0.08)	0.25(0.09)	0.02(0.11)
sys $\mathcal{O}(a^2/L)$	4.43(1.38)	3.49(1.37)	1.08(1.57)
sys strange con	0.30	0	0.30
sys sub-discon	0	0.50	0.50
sys all	5.11(1.32)	3.99(1.29)	1.77(1.13)

**Table 2:** Central value and various systematic errors, use the hybrid continuum limit for the connected diagrams. Numbers in parentheses are statistical error for the corresponding values. [33]

- Sum over time component for  $x_{\text{op}}$ .
- Only sum over  $r = x - y$ .

Finally a small trick is used to reorder summation for  $x, y, z$  so that  $|x - y| \leq \min(|y - z|, |x - z|)$  for the connected diagram. The method is tested in pure QED by calculating the muon leptonic light-by-light contribution to muon  $g - 2$ , where we replace the quark loop in HLbL by a muon loop. The calculation is performed with three different volume and each with three different lattice spacings. As is shown in Figure 6, after the continuum and infinite volume extrapolation via the following the fit form, the known analytical result is obtained.

$$a_\mu(L, a) = a_\mu \left( 1 - \frac{b_2}{(m_\mu L)^2} + \frac{b_3}{(m_\mu L)^3} \right) \left( 1 - c_1(m_\mu a)^2 + c_2(m_\mu a)^4 \right). \quad (8)$$

The method can also be applied to the disconnected diagrams. [39] For most lattice ensembles, 1024 point source quark propagators is calculated, they form  $1024^2$  different point pairs, and each pair is used in the calculation to beat down the statistical error of the disconnected diagrams.

For the calculation by RBC-UKQCD [33], the lattice ensembles used in the lattice is listed in Table 1. Möbius domain wall fermion action is used in the calculation. Pion mass parameters in all the ensembles are very close to its physical value. As seen in Figure 7, which shows the cumulative sum of all contributions up to a given separation of the two sampled currents in the hadronic loop, the total connected contribution saturates at a distance of about 1 fm for all ensembles. This suggests the region  $r > 1$  fm adds mostly noise and little signal, and the situation gets worse in the continuum limit. To reduce this source of statistical error, the statistically more precise 48I results of the contribution from this  $r > 1$  fm region is used to approximate the 64I results of the same region. An estimate of the systematic error on this long distance part is included as “sys hybrid  $\mathcal{O}(a^2)$ ” in Table 2. Extrapolations to the continuum and infinite volume is performed similarly to the QED test with the following fit form.

$$a_\mu(L, a^I, a^D) = a_\mu \left( 1 - \frac{b_2}{(m_\mu L)^2} - c_1^I (a^I \text{ GeV})^2 - c_1^D (a^D \text{ GeV})^2 + c_2^D (a^D \text{ GeV})^4 \right) \quad (9)$$

The result of the fit is shown in Figure 8. The final results for the connected diagrams, disconnected diagrams, total (the sum of the connected diagram and diagram) and estimations of the systematic error due to missing higher order terms in the fit form and other sources are summarized in Table 2.

### 3. QED $_{\infty}$ approach

The QED $_{\infty}$  approach is pioneered by the Mainz group. [34, 41–43] The main idea is to evaluate the QED part of the HLbL diagrams, including the photon and the muon propagator, in infinite volume (semi-)analytically. This QED kernel function can be evaluated beforehand and saved to disk. The 4 dimensional Euclidean space time rotation symmetry can be exploited in the calculation of the QED kernel and also help combine with the hadronic part to obtain the HLbL contribution to muon  $g - 2$ . Due to the current conservation condition, one can perform appropriate subtractions to the QED kernel without change the final result, but may reduce the statistical error as well as reducing the effects caused by discretization and finite volume. [34, 45]

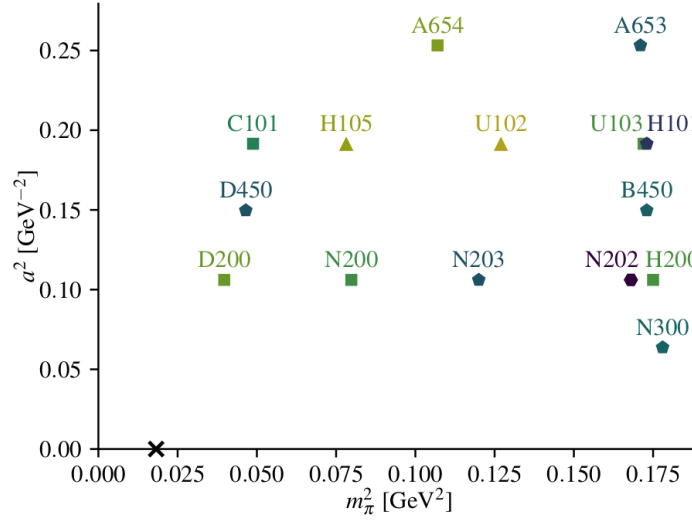


**Figure 9:**  $O(a)$ -improved Wilson fermion ensembles generated by the CLS initiative. [44] The small cross symbol represent the physical point.

Contribution	Value $\times 10^{11}$
Light-quark fully-connected and (2 + 2)	107.4(11.3)(9.2)(6.0)
Strange-quark fully-connected and (2 + 2)	-0.6(2.0)
(3 + 1)	0.0(0.6)
(2 + 1 + 1)	0.0(0.3)
(1 + 1 + 1 + 1)	0.0(0.1)
Total	106.8(15.9)

**Table 3:** A breakdown of the Mainz HLbL result. [34]

The calculation uses the  $O(a)$ -improved Wilson fermion ensembles generated by the CLS initiative [44] as illustrated in Figure 9. Different lattice spacings, lattice sizes, and pion masses are



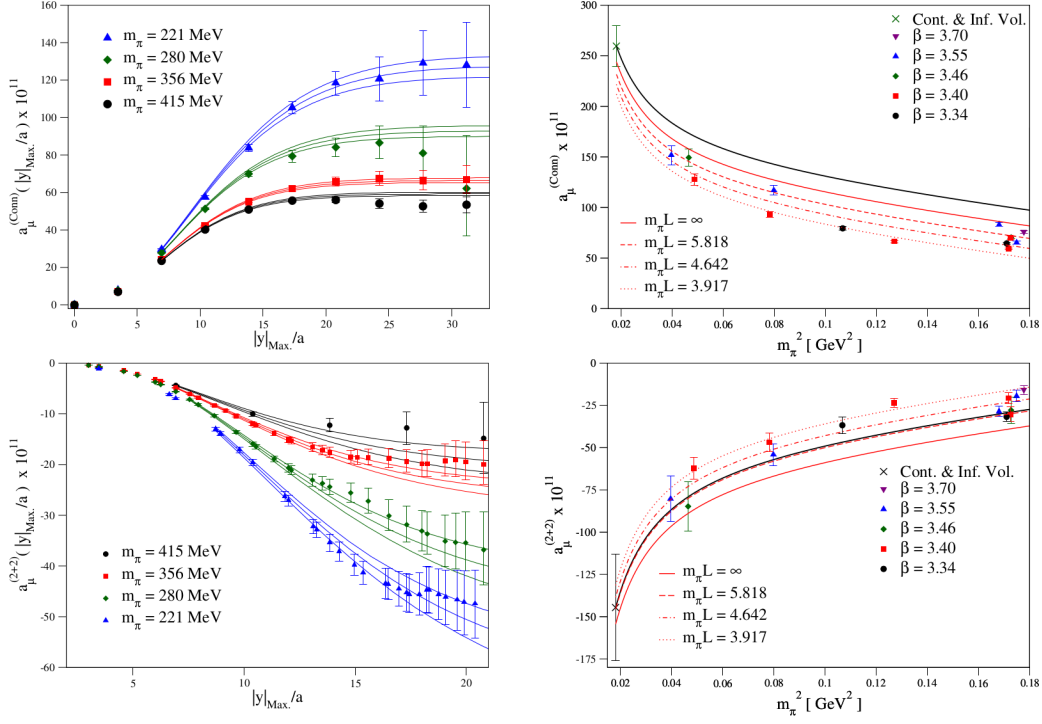


**Figure 10:** The cumulative sum (left) and the extrapolation to the physical point (right) for the connected diagram (upper) and disconnected diagram (lower). [34]

used to allow extrapolation to the physical point. Similar to the  $\text{QED}_L$  calculation, two point source propagators are used to evaluate the connected and the disconnected diagram. The cumulative sum as a function of the separation of the two point source locations is plotted in Figure 10 on the left. It should be noted that the integrand depends on the subtraction scheme for the QED kernel used. [34, 45] To reduce the statistical error from the long distance region, the long distance part of the integrand is fitted using a simple empirical ansatz. The result is then extrapolated to the physical point as plotted in Figure 10 on the right. Due to the pion pole contribution, the connected diagram and the disconnected diagram individually has strong pion mass dependence especially when pion mass is small. However, this strong pion mass largely cancel and the sum only have relatively weak pion mass dependence as shown in Figure 11, where the result is consistent with linear in  $m_\pi^2$ .

The systematic errors from the discretization effects and the effects of excluding the  $m_\pi^2 < 0.165 \text{ GeV}$  or  $m_\pi L < 4$  ensembles in the fit are studied. While the CLS ensemble is  $O(a)$ -improved, the vector current operator used in the calculation is not improved and may generate some  $O(a)$  discretization error. Therefore, both  $O(a)$  and  $O(a^2)$  extrapolation is studied and the difference is the main source of the systematic errors. A different fit form of the pion mass dependence is tried for the Chiral extrapolation of the final result. Half difference,  $6.0 \times 10^{-11}$ , is used as an estimate of the systematic error due to the Chiral extrapolation. The final result is shown in Table 3.

In addition to the HLbL contribution to muon  $g - 2$ , the hadronic light-by-light scattering amplitude in various kinetic setup is also studied by the Mainz group. [42, 43]

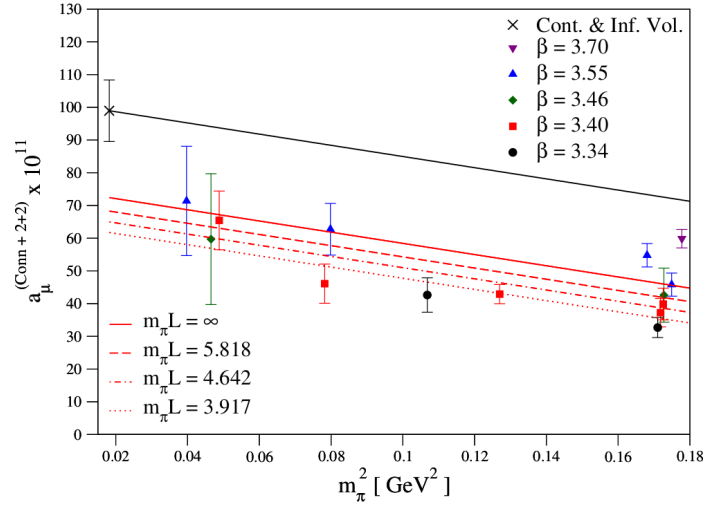


**Figure 11:** Extrapolation of the sum of the connected and disconnected diagrams to the physical point. [34]

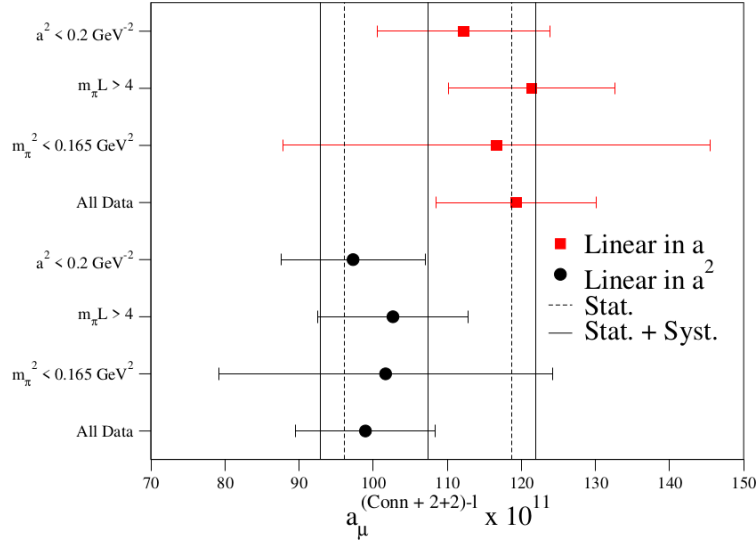


**Figure 12:** Systematic uncertainty of the continuum extrapolation. Root-mean-squared deviation ( $9.2 \times 10^{-11}$ ) is estimated to be the uncertainty. [34]

#### 4. Summary

The current status of the HLbL contribution is summarized in Figure 13. Mainz 2021 [34] is the most recent lattice result. It uses heavier pion mass with infinite volume QED kernel and extrapolate to the physical pion mass. RBC-UKQCD 2019 [33] is the first lattice result with all systematic errors under control. It uses physical pion mass in the finite volume QED<sub>L</sub> scheme and extrapolate to the infinite volume. WP 2020 result [2] is the result from the data-driven analytical approach summarized in the white paper. It is the sum of the contributions from different cuts and poles. High energy contributions are the major source of uncertainties. All these three

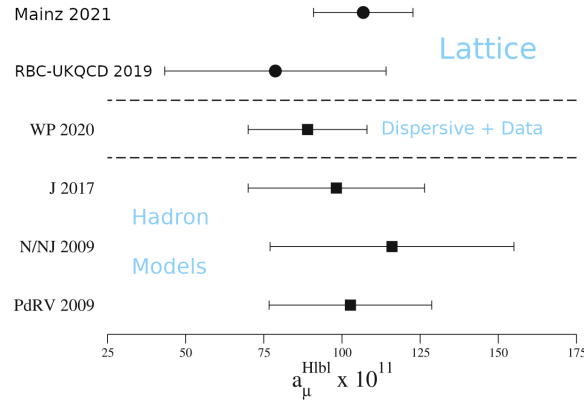


**Figure 13:** HLbL summary.

results have different systematics and agree well with each other. Uncorrelated average gives:  $a_{\mu}^{\text{HLbL}} = 97.7(11.6) \times 10^{-11}$ . At this point, it is safe to conclude that the hadronic light-by-light (HLbL) contribution cannot be the source of the muon  $g - 2$  puzzle. Further improvements in precision for both lattice method and the analytical approaches are still underway to match with the Fermilab's final precision goal.

## Acknowledgments

The author thank the following from RBC-UKQCD collaborations and Mainz group for willingly sharing their results and discussing their work: N. Asmussen, T. Blum, N. Christ, A. Gerardin, M. Hayakawa, T. Izubuchi, C. Jung, C. Lehner, H. B. Meyer, A. Nyffeler. L.C.J. acknowledges support by DOE Office of Science Early Career Award DE-SC0021147 and DOE grant DE-SC0010339.

## References

- [1] J. S. Schwinger, Phys. Rev. **73**, 416-417 (1948) doi:10.1103/PhysRev.73.416
- [2] T. Aoyama, N. Asmussen, M. Benayoun, J. Bijnens, T. Blum, M. Bruno, I. Caprini, C. M. Carloni Calame, M. Cè and G. Colangelo, *et al.* Phys. Rept. **887**, 1-166 (2020) doi:10.1016/j.physrep.2020.07.006 [arXiv:2006.04822 [hep-ph]].
- [3] T. Aoyama, M. Hayakawa, T. Kinoshita and M. Nio, Phys. Rev. Lett. **109**, 111808 (2012) doi:10.1103/PhysRevLett.109.111808 [arXiv:1205.5370 [hep-ph]].
- [4] C. Gnendiger, D. Stöckinger and H. Stöckinger-Kim, Phys. Rev. D **88**, 053005 (2013) doi:10.1103/PhysRevD.88.053005 [arXiv:1306.5546 [hep-ph]].
- [5] G. W. Bennett *et al.* [Muon  $g-2$ ], Phys. Rev. D **73**, 072003 (2006) doi:10.1103/PhysRevD.73.072003 [arXiv:hep-ex/0602035 [hep-ex]].
- [6] B. Abi *et al.* [Muon  $g-2$ ], Phys. Rev. Lett. **126**, no.14, 141801 (2021) doi:10.1103/PhysRevLett.126.141801 [arXiv:2104.03281 [hep-ex]].

- [7] T. Albahri *et al.* [Muon  $g-2$ ], Phys. Rev. D **103**, no.7, 072002 (2021) doi:10.1103/PhysRevD.103.072002 [arXiv:2104.03247 [hep-ex]].
- [8] T. Albahri *et al.* [Muon  $g-2$ ], Phys. Rev. A **103**, no.4, 042208 (2021) doi:10.1103/PhysRevA.103.042208 [arXiv:2104.03201 [hep-ex]].
- [9] T. Albahri *et al.* [Muon  $g-2$ ], Phys. Rev. Accel. Beams **24**, no.4, 044002 (2021) doi:10.1103/PhysRevAccelBeams.24.044002 [arXiv:2104.03240 [physics.acc-ph]].
- [10] T. Mibe [J-PARC  $g-2$ ], Chin. Phys. C **34**, 745-748 (2010) doi:10.1088/1674-1137/34/6/022
- [11] M. Otani [J-PARC muon  $g - 2$ /EDM C], PoS **NuFact2021**, 139 (2022) doi:10.22323/1.402.0139
- [12] J. Prades, E. de Rafael and A. Vainshtein, Adv. Ser. Direct. High Energy Phys. **20**, 303-317 (2009) doi:10.1142/9789814271844\_0009 [arXiv:0901.0306 [hep-ph]].
- [13] A. Nyffeler, Phys. Rev. D **79**, 073012 (2009) doi:10.1103/PhysRevD.79.073012 [arXiv:0901.1172 [hep-ph]].
- [14] F. Jegerlehner and A. Nyffeler, Phys. Rept. **477**, 1-110 (2009) doi:10.1016/j.physrep.2009.04.003 [arXiv:0902.3360 [hep-ph]].
- [15] G. Colangelo, M. Hoferichter, M. Procura and P. Stoffer, JHEP **09**, 091 (2014) doi:10.1007/JHEP09(2014)091 [arXiv:1402.7081 [hep-ph]].
- [16] G. Colangelo, M. Hoferichter, B. Kubis, M. Procura and P. Stoffer, Phys. Lett. B **738**, 6-12 (2014) doi:10.1016/j.physletb.2014.09.021 [arXiv:1408.2517 [hep-ph]].
- [17] G. Colangelo, M. Hoferichter, M. Procura and P. Stoffer, JHEP **09**, 074 (2015) doi:10.1007/JHEP09(2015)074 [arXiv:1506.01386 [hep-ph]].
- [18] P. Masjuan and P. Sanchez-Puertas, Phys. Rev. D **95**, no.5, 054026 (2017) doi:10.1103/PhysRevD.95.054026 [arXiv:1701.05829 [hep-ph]].
- [19] G. Colangelo, M. Hoferichter, M. Procura and P. Stoffer, Phys. Rev. Lett. **118**, no.23, 232001 (2017) doi:10.1103/PhysRevLett.118.232001 [arXiv:1701.06554 [hep-ph]].
- [20] G. Colangelo, M. Hoferichter, M. Procura and P. Stoffer, JHEP **04**, 161 (2017) doi:10.1007/JHEP04(2017)161 [arXiv:1702.07347 [hep-ph]].
- [21] M. Hoferichter, B. L. Hoid, B. Kubis, S. Leupold and S. P. Schneider, Phys. Rev. Lett. **121**, no.11, 112002 (2018) doi:10.1103/PhysRevLett.121.112002 [arXiv:1805.01471 [hep-ph]].
- [22] M. Hoferichter, B. L. Hoid, B. Kubis, S. Leupold and S. P. Schneider, JHEP **10**, 141 (2018) doi:10.1007/JHEP10(2018)141 [arXiv:1808.04823 [hep-ph]].
- [23] A. Gérardin, H. B. Meyer and A. Nyffeler, Phys. Rev. D **100**, no.3, 034520 (2019) doi:10.1103/PhysRevD.100.034520 [arXiv:1903.09471 [hep-lat]].

- [24] J. Bijnens, N. Hermansson-Truedsson and A. Rodríguez-Sánchez, *Phys. Lett. B* **798**, 134994 (2019) doi:10.1016/j.physletb.2019.134994 [arXiv:1908.03331 [hep-ph]].
- [25] G. Colangelo, F. Hagelstein, M. Hoferichter, L. Laub and P. Stoffer, *Phys. Rev. D* **101**, no.5, 051501 (2020) doi:10.1103/PhysRevD.101.051501 [arXiv:1910.11881 [hep-ph]].
- [26] G. Colangelo, F. Hagelstein, M. Hoferichter, L. Laub and P. Stoffer, *JHEP* **03**, 101 (2020) doi:10.1007/JHEP03(2020)101 [arXiv:1910.13432 [hep-ph]].
- [27] P. Achard *et al.* [L3], *JHEP* **03**, 018 (2007) doi:10.1088/1126-6708/2007/03/018
- [28] I. Danilkin, C. F. Redmer and M. Vanderhaeghen, *Prog. Part. Nucl. Phys.* **107**, 20-68 (2019) doi:10.1016/j.pnpnp.2019.05.002 [arXiv:1901.10346 [hep-ph]].
- [29] M. N. Achasov *et al.* [SND], *Phys. Lett. B* **800**, 135074 (2020) doi:10.1016/j.physletb.2019.135074 [arXiv:1906.03838 [hep-ex]].
- [30] I. Larin *et al.* [PrimEx-II], *Science* **368**, no.6490, 506-509 (2020) doi:10.1126/science.aay6641
- [31] M. Ablikim *et al.* [BESIII], *Chin. Phys. C* **44**, no.4, 040001 (2020) doi:10.1088/1674-1137/44/4/040001 [arXiv:1912.05983 [hep-ex]].
- [32] M. Hoferichter, *EPJ Web Conf.* **258**, 06004 (2022) doi:10.1051/epjconf/202225806004
- [33] T. Blum, N. Christ, M. Hayakawa, T. Izubuchi, L. Jin, C. Jung and C. Lehner, *Phys. Rev. Lett.* **124**, no.13, 132002 (2020) doi:10.1103/PhysRevLett.124.132002 [arXiv:1911.08123 [hep-lat]].
- [34] E. H. Chao, R. J. Hudspith, A. Gérardin, J. R. Green, H. B. Meyer and K. Ottnad, *Eur. Phys. J. C* **81**, no.7, 651 (2021) doi:10.1140/epjc/s10052-021-09455-4 [arXiv:2104.02632 [hep-lat]].
- [35] T. Blum, S. Chowdhury, M. Hayakawa and T. Izubuchi, *Phys. Rev. Lett.* **114**, no.1, 012001 (2015) doi:10.1103/PhysRevLett.114.012001 [arXiv:1407.2923 [hep-lat]].
- [36] M. Hayakawa, T. Blum, T. Izubuchi and N. Yamada, *PoS LAT2005*, 353 (2006) doi:10.22323/1.020.0353 [arXiv:hep-lat/0509016 [hep-lat]].
- [37] M. Hayakawa and S. Uno, *Prog. Theor. Phys.* **120**, 413-441 (2008) doi:10.1143/PTP.120.413 [arXiv:0804.2044 [hep-ph]].
- [38] T. Blum, N. Christ, M. Hayakawa, T. Izubuchi, L. Jin and C. Lehner, *Phys. Rev. D* **93**, no.1, 014503 (2016) doi:10.1103/PhysRevD.93.014503 [arXiv:1510.07100 [hep-lat]].
- [39] T. Blum, N. Christ, M. Hayakawa, T. Izubuchi, L. Jin, C. Jung and C. Lehner, *Phys. Rev. Lett.* **118**, no.2, 022005 (2017) doi:10.1103/PhysRevLett.118.022005 [arXiv:1610.04603 [hep-lat]].
- [40] T. Blum *et al.* [RBC and UKQCD], *Phys. Rev. D* **93**, no.7, 074505 (2016) doi:10.1103/PhysRevD.93.074505 [arXiv:1411.7017 [hep-lat]].

- [41] E. H. Chao, A. Gérardin, J. R. Green, R. J. Hudspith and H. B. Meyer, *Eur. Phys. J. C* **80**, no.9, 869 (2020) doi:10.1140/epjc/s10052-020-08444-3 [arXiv:2006.16224 [hep-lat]].
- [42] A. Gérardin, J. Green, O. Gryniuk, G. von Hippel, H. B. Meyer, V. Pascalutsa and H. Wittig, *Phys. Rev. D* **98**, no.7, 074501 (2018) doi:10.1103/PhysRevD.98.074501 [arXiv:1712.00421 [hep-lat]].
- [43] J. Green, O. Gryniuk, G. von Hippel, H. B. Meyer and V. Pascalutsa, *Phys. Rev. Lett.* **115**, no.22, 222003 (2015) doi:10.1103/PhysRevLett.115.222003 [arXiv:1507.01577 [hep-lat]].
- [44] M. Bruno, D. Djukanovic, G. P. Engel, A. Francis, G. Herdoiza, H. Horsch, P. Korcyl, T. Korzec, M. Papinutto and S. Schaefer, *et al.* *JHEP* **02**, 043 (2015) doi:10.1007/JHEP02(2015)043 [arXiv:1411.3982 [hep-lat]].
- [45] T. Blum, N. Christ, M. Hayakawa, T. Izubuchi, L. Jin, C. Jung and C. Lehner, *Phys. Rev. D* **96**, no.3, 034515 (2017) doi:10.1103/PhysRevD.96.034515 [arXiv:1705.01067 [hep-lat]].